

Amorphous Titanium Sulfide Electrode for All-solid-state Rechargeable Lithium Batteries with High Capacity

Akitoshi Hayashi,* Takuya Matsuyama, Atsushi Sakuda, and Masahiro Tatsumisago

Department of Applied Chemistry, Osaka Prefecture University, 1-1 Gakuen-cho, Naka-ku, Sakai, Osaka 599-8531

(Received April 28, 2012; CL-120373; E-mail: hayashi@chem.osakafu-u.ac.jp)

Amorphous TiS_3 active materials were prepared using a high-energy ball mill and first applied to all-solid-state cells with $\text{Li}_2\text{S-P}_2\text{S}_5$ solid electrolyte. The solid-state cell operated as a rechargeable lithium battery with a high capacity of 400 mA h g^{-1} at room temperature. The cell exhibited a higher capacity than a solid-electrolyte cell with crystalline TiS_2 and showed better cyclability than a liquid-electrolyte cell with crystalline TiS_3 .

Development of rechargeable batteries with high energy density and high safety is desired. Metal sulfides have a relatively high electronic conductivity and high capacity, which are remarkable advantages as an active material for high-rate and high-capacity applications. Crystalline TiS_2 with layer structure is known to show good cyclability in electrochemical cells with organic liquid electrolytes.^{1,2} TiS_2 was also applied to all-solid-state cells with sulfide solid electrolytes and the cells operated at room temperature with excellent cyclability.^{3,4}

Crystalline TiS_3 was also examined as an active material for liquid-electrolyte cells.⁵⁻⁷ TiS_3 has a higher theoretical capacity of 558 mA h g^{-1} than TiS_2 (240 mA h g^{-1}). The TiS_3 cell showed a higher capacity than the TiS_2 cell for initial a few cycles, but the capacity of the TiS_3 cell drastically decreased after the fifth cycle.⁷ The difference in cyclability between TiS_2 and TiS_3 has not been clarified; one possible reason is structural deterioration of TiS_3 crystals during cycles with organic liquid electrolytes.

Amorphization of active materials is potentially capable of achieving higher capacity and cyclability because of the presence of additional stable sites for lithium ions on the basis of open and random structure in amorphous materials. For example, amorphous V_2O_5 exhibits better rechargeability than crystalline V_2O_5 .⁸ The chemical diffusion coefficient of V_2O_5 is also increased by amorphization.

Moreover, applying inorganic solid electrolytes to electrochemical cells has the benefit of potential use of active materials which do not show enough performance in liquid-electrolyte cells. For example, elemental sulfur with a high theoretical capacity (1672 mA h g^{-1}) attracts much attention as a positive electrode for a Li/S battery with a high energy density.⁹ However, the Li/S batteries suffered from rapid capacity fading mainly due to the dissolution of polysulfides, which were formed during charge-discharge processes in the sulfur electrode. On the other hand, all-solid-state Li/S batteries with sulfide solid electrolytes showed excellent cycle performance.^{10,11}

Amorphous TiS_3 has never been electrochemically examined in not only organic liquid electrolytes but also sulfide solid electrolytes. Both high capacity and good cyclability would be achieved by the use of the combination of amorphous TiS_3 and a sulfide solid electrolyte.

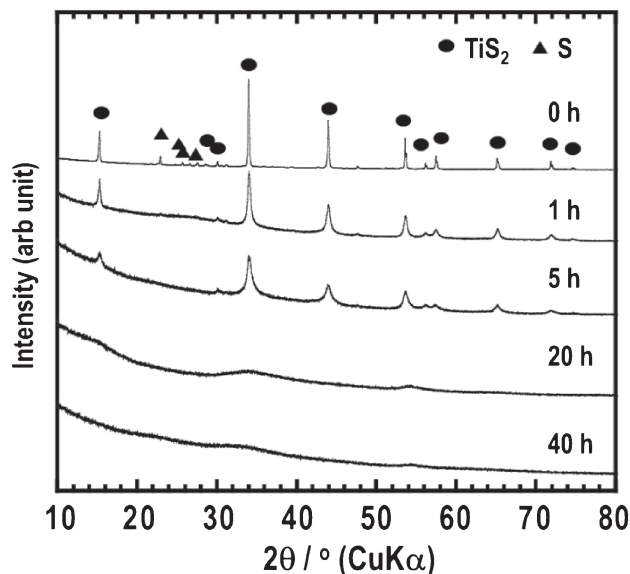


Figure 1. XRD patterns of the equimolar mixtures of crystalline TiS_2 and sulfur, which were ball-milled for several periods of time.

In this study, amorphous TiS_3 was mechanochemically prepared and characterized by X-ray diffraction (XRD), scanning electron microscopy (SEM), differential thermal analysis (DTA), and Raman spectroscopy. The obtained active materials were applied to all-solid-state cells with the $\text{Li}_2\text{S-P}_2\text{S}_5$ electrolytes. Electrochemical performance of the cells was compared to that of a cell using crystalline TiS_2 electrodes.

Amorphous TiS_3 was prepared by ball milling an equimolar mixture of crystalline TiS_2 (99.9%; Kojundo Chem.) and sulfur (99.98%; Aldrich). A zirconia pot (45 mL) with 500 zirconia balls (4 mm in diameter) was used for the experiment, and the rotation speed of a planetary ball mill apparatus (Fritsch P-7) was fixed to 370 rpm. Figure 1 shows XRD patterns of the prepared samples milled for several periods of time. The diffraction peaks attributable to sulfur disappeared by milling for 1 h. On the other hand, the intensity of the peaks attributable to TiS_2 gradually decreased with an increase in the milling time, and a halo pattern was almost dominant after milling for more than 20 h.

The SEM image of the equimolar mixture of TiS_2 and S before milling indicated that the mixture consisted of plate-like TiS_2 particles of ca. 500 nm in size and sulfur particles of ca. 50 μm . The SEM image and EDX maps of S and Ti elements for the sample milled for 40 h are shown in Figure 2.

Secondary particles of several microns in size, which were formed by agglomeration of submicron-sized ordinary particles,

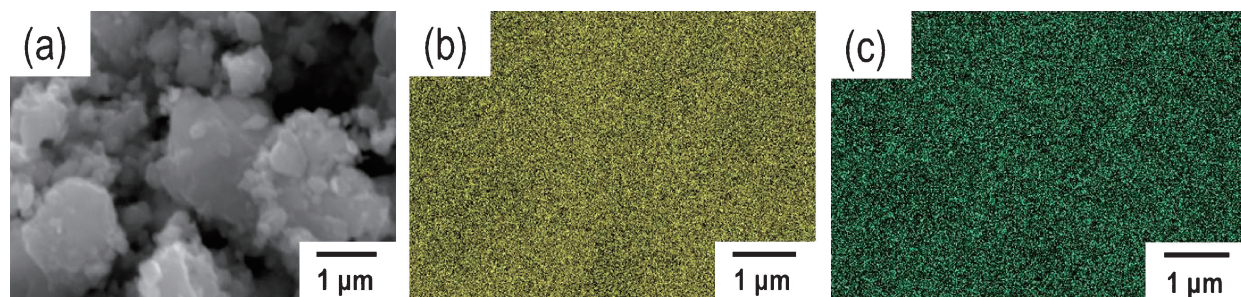


Figure 2. SEM image (a) and EDX maps of S (b) and Ti (c) elements for the the equimolar mixture of crystalline TiS_2 and sulfur milled for 40 h.

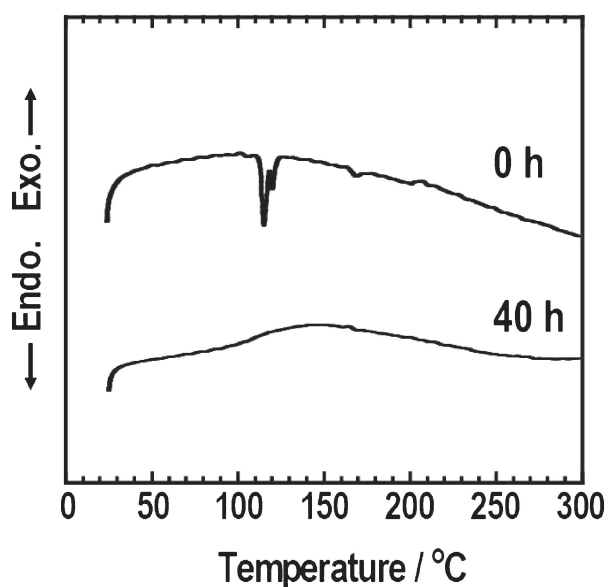


Figure 3. DTA curves of the the equimolar mixtures of crystalline TiS_2 and sulfur milled for 0 or 40 h.

were mainly observed in the SEM image (a). The EDX map of sulfur (b) for the SEM image almost overlapped the map of Ti (c), suggesting that sulfur and TiS_2 particles were not separately present but TiS_x particles were prepared. The DTA curve of the sample milled for 40 h exhibited no endothermic peaks attributable to melt of crystalline sulfur, which were observed at around 115 °C in the equimolar mixture of TiS_2 and S before milling (0 h) as shown in Figure 3. It is noted by XRD, SEM-EDX, and DTA that amorphous TiS_x would be prepared.

Figure 4 shows the Raman spectra of the samples milled for 0 or 40 h. Two broad bands at 335 and 230 cm^{-1} appeared in the Raman spectrum of the sample before milling (0 h); the bands were observed for crystalline TiS_2 , and the band at 230 cm^{-1} was also observed for crystalline sulfur. After milling for 40 h, the intensity of the two bands decreased and two new bands at 375 and 303 cm^{-1} , which were observed for crystalline TiS_3 ,¹² appeared. This suggests that TiS_2 and S reacted to form amorphous TiS_3 , and thus the prepared sample is called amorphous TiS_3 in the following discussion.

The amorphous TiS_3 prepared was applied as an active material to all-solid-state lithium cells. The 80 Li_2S ·20 P_2S_5 (mol%) glass-ceramic electrolyte¹³ was used because of its

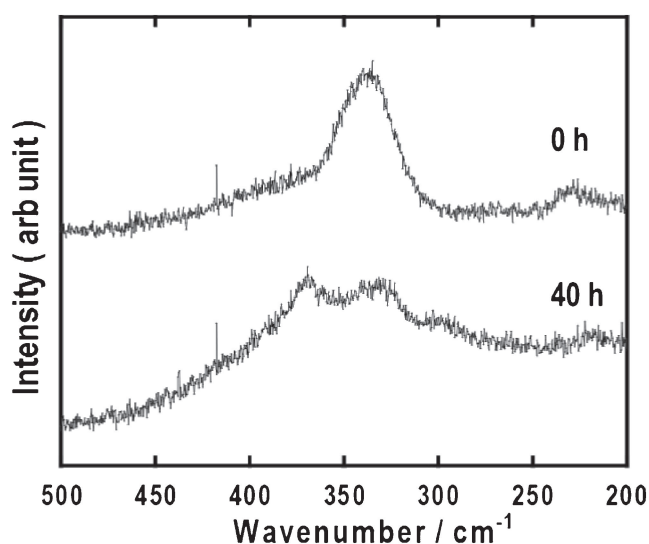


Figure 4. Raman spectra of the the equimolar mixtures of crystalline TiS_2 and sulfur milled for 0 or 40 h.

high lithium ion conductivity of over 10^{-3}Scm^{-1} . A hand-grinding mixture of the TiS_3 , the electrolyte, and acetylene black (conductive additive) with a weight ratio of 40:60:6 was used as a working electrode. A three-layered pellet of the working electrode, the electrolyte, and Li-In alloy (counter electrode) was prepared by uniaxial press at room temperature to form all-solid-state Li-In/ Li_2S - P_2S_5 / TiS_3 cells. Figure 5 shows the initial charge-discharge curves of the all-solid-state cells at 25 °C. Both crystalline TiS_2 and the TiS_2 milled for 40 h were used as active materials for comparison. The inset shows the cycle performance of the cell with the amorphous TiS_3 active material. A current density was 0.064 mA cm^{-2} and a cutoff voltage was 0.9–2.4 V. All the cells worked as a secondary battery at 25 °C. The cell with crystalline TiS_2 exhibited a reversible capacity of ca. 230 mA h g^{-1} , which was close to the theoretical capacity of 240 mA h g^{-1} . Crystalline TiS_2 particles were pulverized by milling for 40 h (not to be amorphous), but the cell with the milled TiS_2 exhibited a similar charge-discharge profile to the cell with crystalline TiS_2 without milling-treatment. On the other hand, the amorphous TiS_3 prepared by milling of the equimolar mixture of TiS_2 and S for 40 h showed a higher capacity of ca. 400 mA h g^{-1} than the TiS_2 electrodes. As shown in the inset, the all-solid-state cell with the amorphous TiS_3 retained over 300 mA h g^{-1} after 10 cycles.

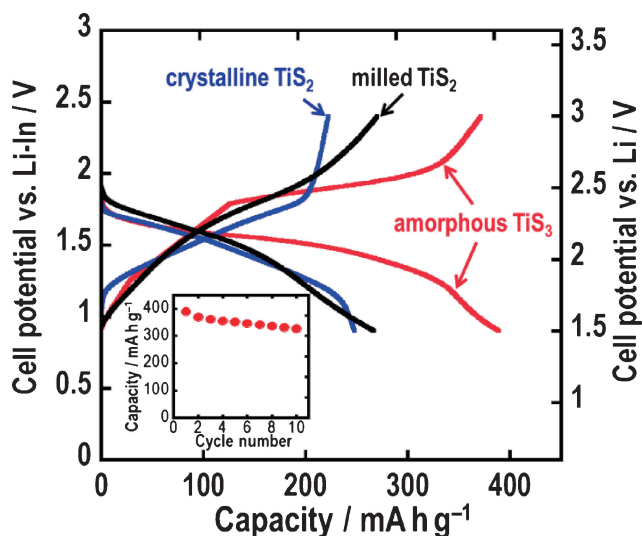


Figure 5. Initial charge–discharge curves of the all-solid-state Li–In/Li₂S–P₂S₅/TiS_x cells at 25 °C. The inset shows the cycle performance of the cell with the amorphous TiS₃ active material.

The cyclability of the TiS₃ electrode mentioned above was compared to that of a cell with an organic liquid electrolyte. Crystalline TiS₃ active material showed the initial discharge capacity of ca. 350 mA h g⁻¹ at 0.003 mA cm⁻², but its capacity rapidly decreased after several cycles, and a limited capacity of ca. 50 mA h g⁻¹ was only obtained after 10 cycles.⁷ Compared to the liquid electrolyte cell, the amorphous TiS₃ electrode in the all-solid-state cell with the sulfide solid electrolyte exhibited the higher capacity and better cyclability at 0.064 mA cm⁻² as mentioned above. The average operating voltages of the two cells were comparable, suggesting that a similar electrochemical reaction basically occurred during charge–discharge processes. The excellent electrochemical performance observed in the solid-state cell would be brought about by the use of inorganic sulfide electrolytes and/or amorphization of TiS₃ active material. The origin of improving cyclability and capacity of the solid-state cell has not been clarified at the present stage. One

approach to elucidate the origin is the application of crystalline TiS₃ to all-solid-state cells, and this will be demonstrated in the near future.

In conclusion, the amorphous TiS₃ was prepared by ball milling from crystalline TiS₂ and S. The all-solid-state cell with the amorphous TiS₃ electrode and the Li₂S–P₂S₅ electrolyte kept a high capacity of 300 mA h g⁻¹ for 10 cycles at 25 °C. Amorphization of sulfur-rich transition-metal sulfides is useful for achieving active materials with high capacity as well as good cyclability.

This work was carried out with financial support from the Japan Science and Technology Agency (JST), Core Research for Evolutional Science and Technology (CREST) Project.

References

- 1 M. S. Whittingham, *Prog. Solid State Chem.* **1978**, *12*, 41.
- 2 C. M. Julien, *Mater. Sci. Eng., R* **2003**, *40*, 47.
- 3 K. Iwamoto, N. Aotani, K. Takada, S. Kondo, *Solid State Ionics* **1994**, *70–71*, 658.
- 4 J. E. Trevey, C. R. Stoldt, S.-H. Lee, *J. Electrochem. Soc.* **2011**, *158*, A1282.
- 5 G. L. Holleck, J. R. Driscoll, *Electrochim. Acta* **1977**, *22*, 647.
- 6 Y. Ōnuki, R. Inada, S. Tanuma, S. Yamanaka, H. Kamimura, *Solid State Ionics* **1983**, *11*, 195.
- 7 M. H. Lindic, H. Martinez, A. Benayad, B. Pecquenard, P. Vinatier, A. Levasseur, D. Gonbeau, *Solid State Ionics* **2005**, *176*, 1529.
- 8 N. Machida, R. Fuchida, T. Minami, *J. Electrochem. Soc.* **1989**, *136*, 2133.
- 9 X. Ji, L. F. Nazar, *J. Mater. Chem.* **2010**, *20*, 9821.
- 10 N. Machida, K. Kobayashi, Y. Nishikawa, T. Shigematsu, *Solid State Ionics* **2004**, *175*, 247.
- 11 M. Nagao, A. Hayashi, M. Tatsumisago, *Electrochim. Acta* **2011**, *56*, 6055.
- 12 D. W. Galliardt, W. R. Nieveen, R. D. Kirby, *Solid State Commun.* **1980**, *34*, 37.
- 13 A. Hayashi, S. Hama, T. Minami, M. Tatsumisago, *Electrochem. Commun.* **2003**, *5*, 111.